Modeling the Sea Currents in Open Basins: The Case Study for the Hawaiian Island Region

V. G. Bondur[a], R. A. Ibrayev[b], Yu. V. Grebenyuk[a], and G. A. Sarkisyan[c]

[a] Scientific Center of Aerospace Monitoring Aerokosmos, Gorokhovskii per. 4, Moscow, 105064 Russia
e-mail: vgbondur@online.ru
[b] Institute of Numerical Mathematics, Russian Academy of Sciences, ul. Gubkina 8, Moscow, 119991 Russia
e-mail: ibrayev@inm.ras.ru
[c] Shirshov Institute of Oceanology, Russian Academy of Sciences, Nakhimovskii pr. 36, Moscow, 117997 Russia
e-mail: sarkis@inm.ras.ru
Received November 10, 2006; in final form, October 3, 2007

Abstract—The fields of currents in open basins are studied with the use of a mathematical model of ocean hydrodynamics. The area of the Hawaiian Islands is taken as an example. The model, based on three-dimensional equations of thermohydrodynamics, is solved for a domain with open boundaries, at which adaptive boundary conditions are set. We analyze the results of numerical experiments with given monthly mean climatic conditions at the ocean surface and open lateral boundaries with consideration for tides M_2 and K_1. A comparison of the model solutions and observational data shows that the model can realistically reproduce the mean parameters of the ocean state and their variability. The model solutions for the given area were found to have a northward current in the upper oceanic layer. This current clearly manifests itself in averaged fields. The characteristics of averaged currents indicate that the upper 100–150-m layer between the islands of Hawaii and Maui as well as between the islands of Molokai and Oahu is characterized by water transport from the west to the east side of the ridge of islands. The results obtained and the model proposed can be used to monitor physical fields of the ocean.

INTRODUCTION

In monitoring physical fields of the ocean, along with modern technology (including aerospace facilities), the methods of mathematical modeling play an important role [1]. These methods can be efficiently used for studies in ocean physics, for estimation of anthropogenic impacts on ocean water areas, for predicting the pollutant transport under the effect of different factors (currents, wind, diffusion, etc.), for analysis of the possible scenarios of these processes under various hydrometeorological conditions, as well as for assessing the consequences of these impacts on the state of the water areas. To solve these problems, it is important to simulate the water circulation in open basins.

This paper presents simulation results for the fields of currents around the Hawaiian Islands. Such investigations are necessary for a number of applications related to economic activities on island shelves. The study was part of an international project of complex monitoring of anthropogenic impacts on the ecosystems of coastal water areas of the Hawaiian Archipelago [2].

The aim of this paper is, first, to construct a model for the main characteristics of large- and synoptic-scale current variations in the area of the Hawaiian Islands and, second, to reveal quasi-constant and time-varying currents. A successful simulation of the fields of currents around the islands would provide a suitable resolution of the dynamics of synoptic eddies and jet currents on the shelf slope and between the islands, as well the reproduction of the vertical structure of thermohaline fields. Since it is practically impossible to perform calculations with a horizontal resolution of about 1 to 10 km using a model of the entire Pacific, the model treats the small area of the Hawaiian Islands with open boundaries. The influence of large-scale oceanic factors on the water circulation in the area of islands was taken into account by changing thermohaline conditions at open boundaries.

1. SPECIFIC FEATURES OF THE SUBJECT

The subject of this study is open basins of the ocean. As examples, we take the mid-Pacific water areas near the Hawaiian Islands.

The archipelago of the Hawaiian Islands, which are peaks of the subsurface Hawaiian Ridge, is located in the central Pacific. The large-scale features of the circulation in the area of islands are controlled by the fact that this area is located in the northern periphery
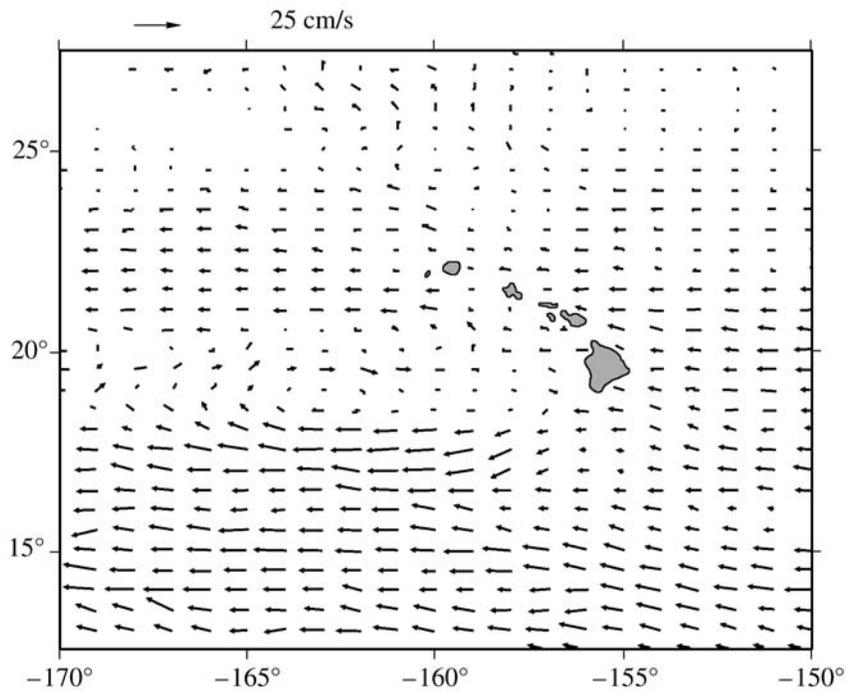
Fig. 1. Mean surface currents in the the Hawaiian Island region from analysis of available current measurements [14].

of the westward North Equatorial Current (NEC) [3, 4]. To the east of the island of Hawaii, the NEC is separated: the northern branch becomes the North Hawaiian Ridge Current, which is northwestward along the Hawaiian Ridge. This current intensifies along the islands, its width is between 75 and 100 km, and the velocity of the surface current with respect to horizons 100–400 dbar is 0.45 m/s [5]. On the basis of field measurements, it has been shown that the current along the Hawaiian Ridge is significantly affected by mesoscale eddies [6, 7]. It was assumed that the existence of a constant current along the ridge cannot be proved. However, long-term observations of currents at a section north of Oahu with acoustic Doppler current profilers (ADCPs) [8, 9] have indicated that the Northern Current of the Hawaiian Ridge does exist. The mean NHRC in the core at a level of 40–90 m reaches 0.17 m/s and, then, decreases significantly with depth. Time series have shown that the current velocity is highly variable.

When flowing about the Hawaiian Islands in the zone from 18° to 22°N, the NEC undergoes deformation. The mean velocity of the NEC current at 13°N is 0.17 m/s; south of the Hawaiian Islands, this value reaches 0.25 m/s [10].

A more detailed review of earlier studies of the dynamics of currents in this area can be found in [11]. The researchers revealed a large number of relatively small cyclonic eddies to the west, which decay on the leeward side of the island of Hawaii. They also describe anticyclonic eddies that are larger in size than

the cyclonic eddies occurring to the south of the island of Hawaii. The eddies are moving westward. This pattern can be confirmed by the trajectory of WOCE-run drifter 6873 [12]. This drifter was uniformly moving westward with a velocity of 0.10 to 0.15 m/s. On passing the southern end of the island of Hawaii, the drifter was captured by an anticyclonic vortex with a diameter of about 100 km. The vortex was moving westward with a velocity of 0.06 m/s.

Conducted on the basis of TOPEX/Poseidon space altimetric data, analysis of the trajectories of anticyclonic eddies emerging when the NEC flows around the island of Hawaii from the south showed that the eddies move initially westward and southwestward and, then, reaching 180°W, normally move northwestward [13]. There is a sufficiently clear boundary west of the island of Hawaii between the areas with prevailing cyclonic eddies (in the north) and the areas with anticyclonic eddies (in the south) [11]. The structure of averaged surface currents west of the islands is characterized by two zonally elongated gyres separated from each other by the Hawaiian Lee Counter Current, located at 19°N and from 170° and 158°E (see Fig. 1).

Being the boundary between the pair of cyclonic and anticyclonic eddies on the chart of averaged currents, the Hawaiian Lee Counter Current (HLCC) manifests itself as the result of a superposition of westward-propagating eddies generated in the leeward side of the Hawaiian Islands.

In this study, we simulate the field of currents in the area of the Hawaiian Archipelago by using a mathematical model of ocean hydrodynamics.

2. MODEL OF OCEAN HYDRODYNAMICS

The numerical model used in this study is an ocean hydrodynamic model with a free surface, based on primitive nonlinear equations of geophysical fluid dynamics in the hydrostatic, Boussinesq, and incompressible-fluid approximations [15–17] (see the Appendix).

The state of ocean hydrodynamics is described by three-dimensional functions of temperature, salinity, and components of flow velocity, as well as a two-dimensional function of the sea surface height. To reconstruct the large-scale ocean circulation, a hydrodynamic model of the sea has been developed [18–20]. In its subsequent version, the model of the inner sea [21] incorporates a description of the interaction between the near-water atmospheric boundary layer and the sea surface, the moisture flux through the atmosphere–ocean interface, their influence on the processes of salination and desalination of the sea-surface layer, and an improved parametrization of turbulent mixing processes.

3. FORMULATION OF THE PROBLEM

The problem is posed to reproduce the variability of the water circulation in an open basin. An example of the area of the Hawaiian Islands under varying conditions at the ocean surface and at open boundaries of the area, including the factor of tides, is considered.

The model domain covers an area around the Hawaiian Islands and is limited by the coordinates from 170° to 150°W and from 15° to 25°N. The horizontal resolution of the model grid is 4' × 4' (about 7.5 × 7.5 km) and allows us to describe only eight large islands, large oceanic eddies, and currents between islands. The model includes 21 vertical levels fixed at depths of 2, 6, 10, 15, 25, 35, 45, 55, 65, 80, 100, 125, 150, 200, 400, 750, 1100, 1500, 2000, 3000, and 4000 m. The maximum depth of the ocean is 4500 m. The model topography is based on the ETOPO2 database [22].

The spatial scale of synoptic inhomogeneities in the given area is determined, among others, by the Rossby baroclinic radius, which is approximately 60 km outside the western boundary layer of the islands [9]. Clearly, the horizontal resolution used in the model makes it possible to describe synoptic eddies and jet currents with a width of more than 30–40 km.

The initial condition in the model is specified by the state of rest and multiyear monthly mean distribution of temperature and salinity. The model equations are integrated until a quasi-periodic solution is reached.

The initial three-dimensional data on the distribution of temperature and salinity were taken from the WOA2001 [23]. The distributions of property fluxes at the atmosphere–ocean interface were taken from [24]. These are monthly mean values for the period between 1979 and 1993 that are calculated from the ERA15 ECMWF data [25]. We have used the fluxes of heat, precipitation, evaporation, and momentum. The heat flux is represented as the sum of shortwave solar radiation penetrating into the ocean, longwave outgoing radiation, and sensible and latent heat fluxes.

In the model domain, the four boundaries (northern, eastern, southern, and western) are open. The external (to the model domain) conditions for the equations of heat and salinity were specified on the basis of climatic data arrays of monthly mean fields of T and S.

During simulations, it is important to reasonably describe the tidal currents. There are a sufficiently large number of ocean-dynamics models describing these currents. In global models, the tidal forces are included into the terms of pressure gradients in the equations of motion. In regional models, the tides are often simulated through the boundary conditions. In this paper, we specify tides through a change in the barotropic components of velocity at open boundaries. We use the two most energy-carrying components of tidal waves. These are the semidiurnal tide M_2 and the diurnal tide K_1, with amplitudes of 0.908 and 0.531, respectively, of the amplitude of the maximum equilibrium tide [26, 27]. The periods of these tides are 12.42 and 23.93 h, respectively. The amplitudes of M_2 and K_1 in the area under study are about 15 cm, and the phase shifts are 30° and 10°, respectively [3]. The external velocities ($\mathbf{v}^{\mathrm{ext}}$) of currents are given as the sum of the quasi-geostrophic and tidal components:

$$\mathbf{v}^{\mathrm{ext}}(\lambda, \varphi, z, t) = \mathbf{v}_{qg}(\lambda, \varphi, z, t) + \mathbf{v}_{tides}(\lambda, \varphi, t),$$

where $\mathbf{v}_{qg}(\lambda, \varphi, z, t)$ are the quasi-geostrophic velocities [16], depending on the change of wind, temperature, and salinity; and $\mathbf{v}_{tides}(\lambda, \varphi, t)$ are the barotropic tidal currents.

The tidal components of currents are computed by the formula

$$(u, v)_{tides} = (u_a, v_a)\sin(2\pi t/T + \Delta\varphi),$$

where (u_a, v_a) is the amplitude of tidal oscillations of velocity at the domain boundary, T is the oscillation period, and $\Delta\varphi$ is the phase shift of tidal oscillations between the opposite boundaries of the domain.

The amplitude of tidal oscillations of velocity is computed by the formula [28]

$$u_a = h\sqrt{g/H},$$

where h is the amplitude of tidal oscillations of the ocean surface and g and H are the gravitational acceleration and the ocean depth, respectively.

In the model with open boundaries, there is a problem of holding the mass balance in the domain. In the model with a varying free surface of the sea, the imbalance of the water budget leads to a change in the mean sea surface height. The imbalance may arise both from physical causes (for example, because of the difference between precipitation and evaporation) and from errors in determining the external boundary conditions (geostrophic currents, precipitation, and evaporation). Let us note that the imbalance for a limited area may also be caused by tidal currents. Apparently, for time intervals smaller than the tidal period, the water mass in the domain may be changed; however, on time scales longer than the tidal period, the total mass flux through the open boundaries must be zero. The radiation condition at the open boundaries does not relate to the conservation law for the water mass in the domain and, consequently, the change of the water mass in the domain may be unrealistic [29].

To avoid an unreasonable change in the mean sea surface height, we use an algorithm for reducing the total water balance of the domain to zero [30]. In our model, the water budget of the basin is determined by the advective transport of waters through the open boundaries, evaporation and precipitation at the sea surface. The variation of water mass in the domain is

$$\frac{dM}{dt} = \frac{d}{dt}\left[\iiint_V \rho dV\right] = \iint_{G_0} \rho \mathbf{v}\mathbf{n}dG_0 + \iint_{G_\zeta} W dG_\zeta.$$

We assume that, at each instant, the water mass in the domain can be changed because of tides alone. The imbalance of water flows caused by other reasons is canceled by a correction velocity. Thus, when reducing the total mass balance to zero, we subtract the tidal component from the boundary currents. Let us introduce the correction velocity ($\mathbf{v}^c$) in the direction of the normal to the boundary. Then, the balanced velocity ($\mathbf{v}^{balanced}$) will be represented as $\mathbf{v}^{balanced} = \mathbf{v} - \mathbf{v}_{tides} - \mathbf{v}^c$. To find $\mathbf{v}^c$, we use the equation of mass balance

$$\frac{dM}{dt} = \iint_{G_0} \rho(\mathbf{v} - \mathbf{v}_{tides} - \mathbf{v}^c)\mathbf{n}dG_0 + \iint_{G_\zeta} W dG_\zeta = 0.$$

The correction velocity is

$$\mathbf{v}^c = \left(\iint_{G_0} \rho(\mathbf{v} - \mathbf{v}_{tides})\mathbf{n}dG_0 + \iint_{G_\zeta} W dG_\zeta \middle/ \iint_{G_0} \rho \mathbf{n}dG_0\right).$$

The water balance of the domain was calculated at each time step. In accordance with the calculation results, the correction velocity was about 10^{-5} m/s, which is several orders of magnitude smaller than the physical velocities of currents. This circumstance has

no effect on the spatial structure of the solution, and the mean (over the sea surface and over intervals longer than the tidal period) sea surface height in the domain remains constant in the integration time.

4. CALCULATION OF AVERAGED CHARACTERISTICS

The system of equations was integrated for a 17-year model time. The time needed for a quasi-periodic state of the upper oceanic layer to be reached was about two years, after which the kinetic energy oscillates about the mean state. The time needed for a quasi-periodic state of the deep ocean to be reached was significantly longer than this time for the upper oceanic layer. On average over the volume, the kinetic energy of motions reaches a quasi-equilibrium state after approximately 10 years, while there is a marked intrannual signal (Fig. 2). Hereinafter, we will analyze the ocean characteristics corresponding to the 17th year of model time.

A comparative analysis of model solutions with observational data and with the results obtained with other models is a mandatory condition for assessing the ability of a model to reproduce the variability of the ocean state and for the reliability of model results in those cases when observational data are lacking or cannot be obtained.

For a first step, we consider the averaged characteristics of water circulation in the domain under study. The chart of annual mean surface currents (Fig. 3), obtained with the proposed model, is very consistent qualitatively with observational data (Fig. 1). Note that the chart presented in Fig. 1 is a compilation of data obtained from different platforms and sensors. This chart reflects the averaged characteristics of currents in the upper layer of the ocean. A part of these data was obtained from Lagrangian drifters located at a depth of 15 m [10].

East and south of the Hawaiian Archipelago, the westward and northwestward NEC is dominant. The maximum velocity is observed in its southern part, near the boundaries of the model domain where the wind velocity generating trade-wind currents is a maximum. South of the island of Hawaii, the velocity of currents is about 0.15 m/s. The ridge of islands deflects the NEC northwestward. Yet, the northwestward surface current clearly marked north of 19°N is due to an eastern wind in the area east of the archipelago. When the archipelago is flowed from the northern side, the current is intensified. This is the North Hawaiian Ridge Current (NHRC), with a surface velocity higher than 20 cm/s. Below the Ekman layer, the velocity of the NHRC decreases with depth and, then, increases again. Clearly, this is related to the formation of the baroclinic boundary layer along the islands. The core of this current is located below the surface at a level of 80 m, and the velocity in the core
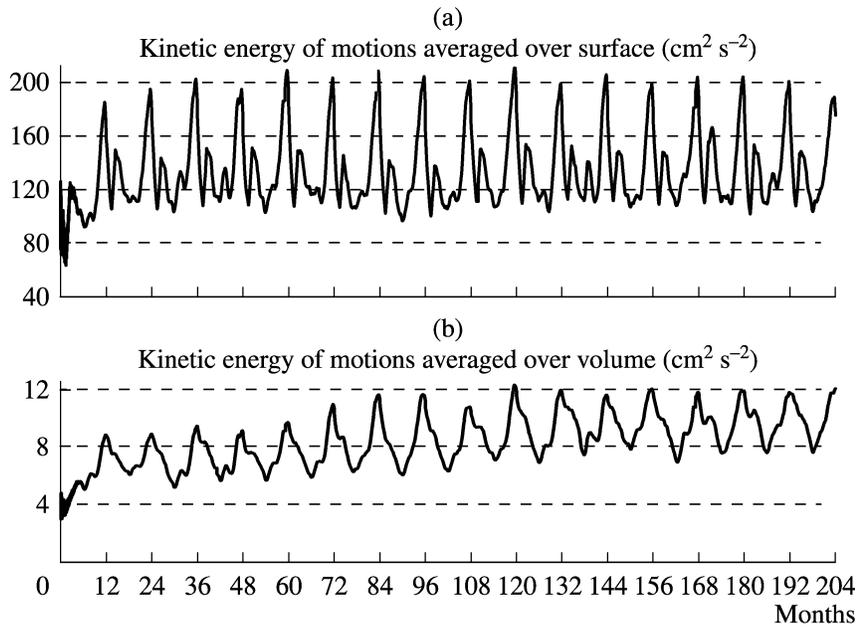
(a)
Kinetic energy of motions averaged over surface (cm² s⁻²)

(b)
Kinetic energy of motions averaged over volume (cm² s⁻²)

Fig. 2. Time series of the kinetic energy of motions ($(u^2 + v^2)/2$) averaged over (a) surface and (b) volume.

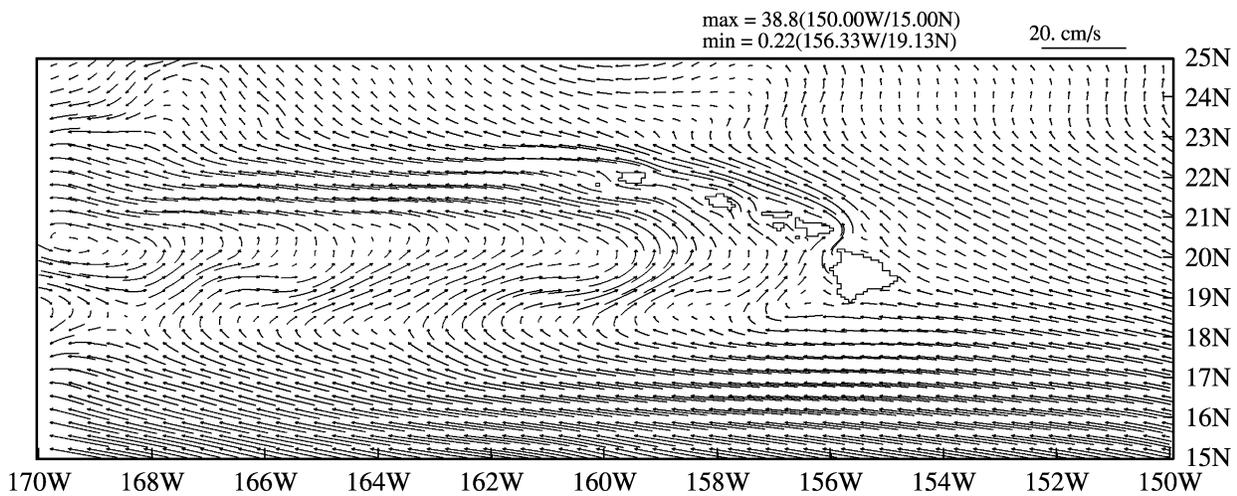max = 38.8(150.00W/15.00N)
min = 0.22(156.33W/19.13N)

20. cm/s

Fig. 3. Streamlines of annual mean currents at a depth of 2 m. The maximum of 38.8 cm/s is reached in the southeastern part of the domain. A model solution.

is about 0.16 m/s (Fig. 4). Let us note that there is a surprising coincidence between this fact and the results of the averaged pattern of currents based on five-year measurements of currents with ADCPs at the section north of the Island of Oahu (see Fig. 5) [8].

In field observational data, the velocity of the NHRC below the core decreases significantly with depth, down to 8 m/s at a depth of 280 m (from data of [8]). The model yields a velocity decrease down to 8 m/s at a level of 350 m (not shown in the figure).

To the west of the archipelago, on the leeward side (in the sense of NEC) the eastward countercurrent is observed in the belt between 19° and 20°N (the Hawaiian leeward countercurrent). In the surface layer, the velocity of gradient currents is affected by the Ekman component of currents, which is induced by tradewinds; therefore, the Hawaiian leeward countercurrent has a northern component of velocity. Below the Ekman layer down to a level between 150 and 200 m, this countercurrent is strictly westward.
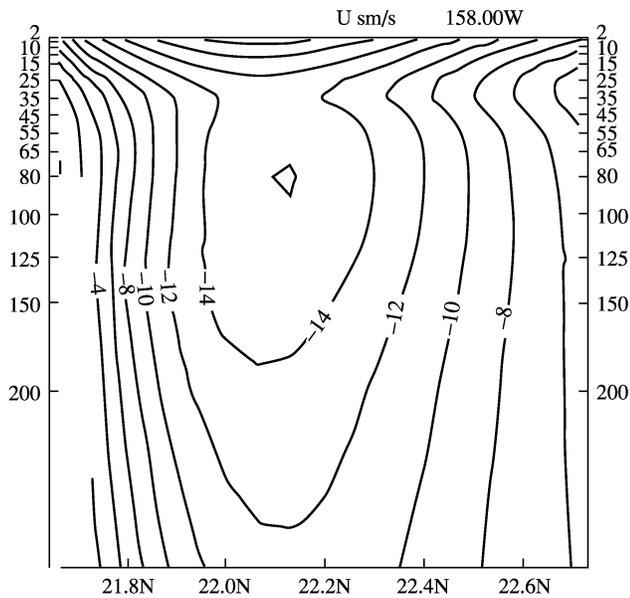
Fig. 4. Meridional section of the zonal component of averaged velocity north of the island of Oahu, along 158°W. Negative values indicate a westward direction. A model solution.

An important difference between the model results and the chart of observed currents is the following. First, in an area 100–200 km west of the islands, in a layer from the surface to a level of about 200 m, there is a northwestward water flow. Second, the model solution indicates that, between the islands of Hawaii and Maui, Molokai and Oahu, in the upper 100–150-m layer, there is transport of waters from the west to the east side of the ridge of islands. Below 200 m, between the islands of Hawaii and Maui, the flow is eastward.

The bottom layer of the ocean has a remarkable cyclonic current enveloping the chain of subsurface ridges at the western boundary of the model domain (Fig. 6). In this area, the currents are stronger than near the Hawaiian Ridge, with their velocities reaching 16 m/s.

The vertical structure of salinity of the upper oceanic layer in this area (Fig. 7) consists of a quasi-uniform layer of increased salinity (34.85 to 35.10‰); a clearly defined halocline, where the salinity decreases rapidly to 34.65‰ at a level of 200 m; and a lower layer of decreased salinity reaching values between 34.3 and 34.4‰. Owing to a high model resolution, the vertical structure of the salinity field is reproduced adequately: it is very consistent with qualitative analyses obtained from observational data.

5. EDDY DYNAMICS IN THE OCEAN

The area west of the Hawaiian Islands is known to generate cyclonic and anticyclonic eddies [11, 31]. The model results confirm the formation of differently directed eddies south of the islands. Properly, the instantaneous pattern of currents in the belt between 18° and 22°N west of the islands has very little in common with the average pattern shown in Fig. 3. The instantaneous field of surface currents is an extremely nonuniform spatial structure (see Fig. 8). Analysis of time series shows that the area south of the latitude 19°N is characterized predominantly by anticyclonic eddies, which are generated by the velocity shear when the island of Hawaii is flowed by the NEC from the south. North of 19°N, cyclonic eddies are predominantly generated.

The temporal evolution of currents can be clearly seen in the plot of longitude–time dependence (the Hofmuller diagram) of the meridional velocity component at a depth of 25 m (Fig. 9). East of the meridian ~156°W, the variation of currents is slight, because the computational domain does not cover the conti-
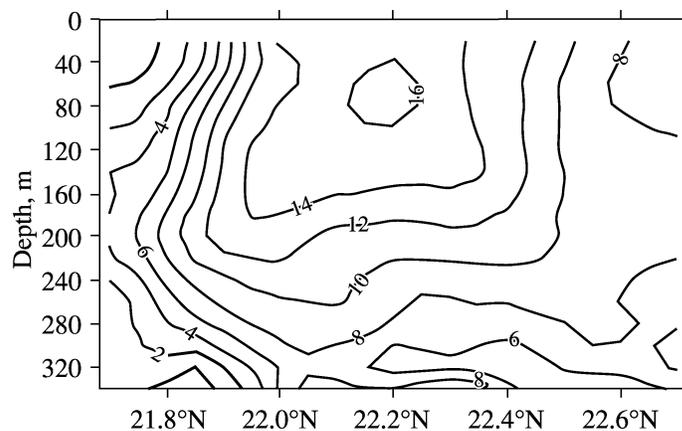

Fig. 5. Vertical profile of averaged velocity across the quasi-meridional section north of the island of Oahu. Positive values of velocity indicate a northwestward direction. The data are averaged over a 5-year period of ADCP measurements [5].
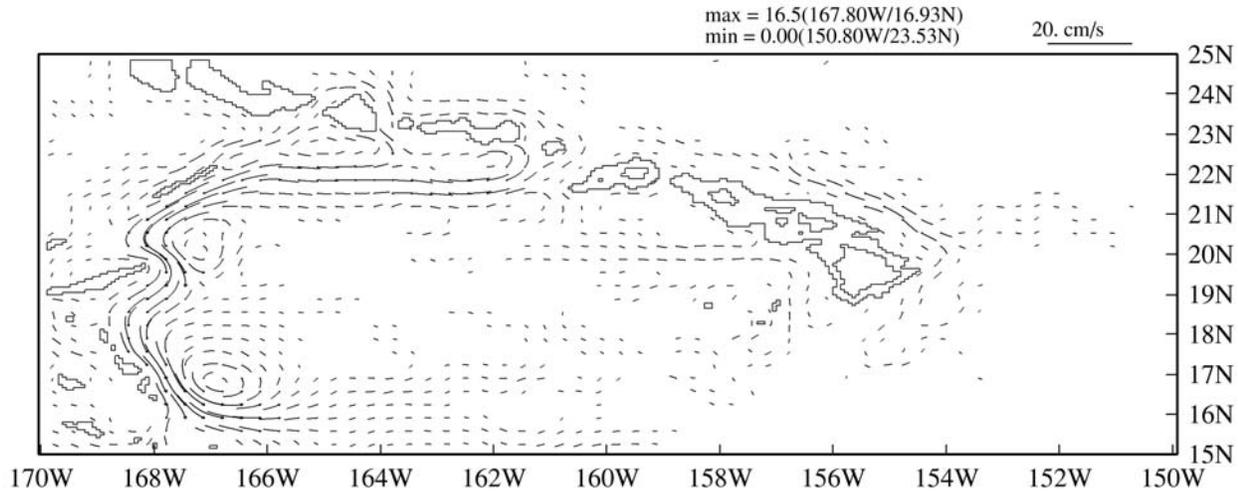
max = 16.5(167.80W/16.93N)
min = 0.00(150.80W/23.53N)   20. cm/s

Fig. 6. Streamlines of annual mean currents at a depth of 3000 m. A maximum of 16.5 cm/s is reached at the point (167.8°W, 16.93°N). A model solution.
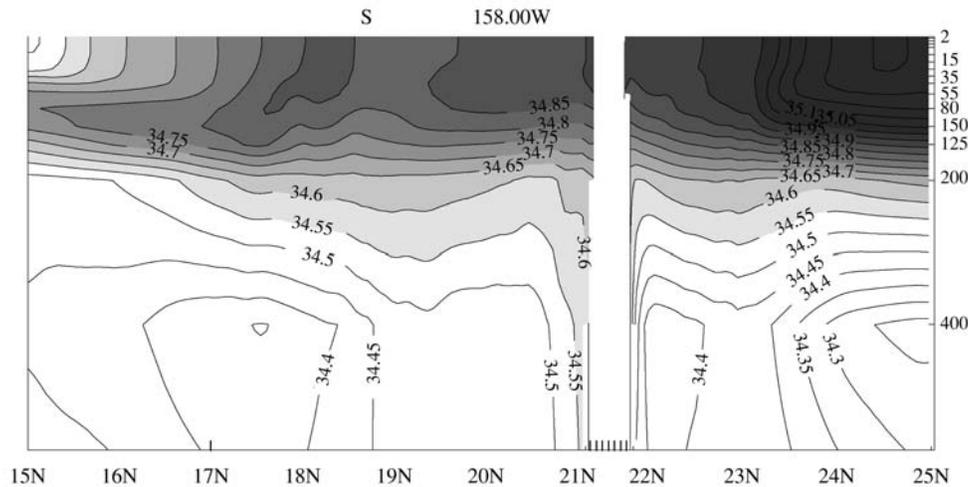

Fig. 7. Meridional section of the annual mean salinity field (ppt) along 158°W. The *Y* axis denotes depth in meters. A model solution.

nental coast, i.e., a possible source of disturbances [12]. Strong disturbances arise at the longitude of the Island of Hawaii ~156°W and move westward. A theoretical estimate, an estimate of the velocity of eddy transport from drifter experimental data, and analysis of altimetric data yield a speed of westward propagation of eddies of about 7 m/s [12]. In the model solution, the propagation speed between 162° and 160°W is approximately 6.4 cm/s. As one moves westward, the velocity of vortex transport falls down to 3.5 cm/s.

8. CONCLUSIONS

In this paper, we have developed a model of thermohydrodynamic processes on a synoptic spatiotemporal scale for open basins. The model is based on a numerical scheme developed in [8, 21]. The open boundaries in the model domain generate a need for setting adaptive boundary conditions [30], based on the equation of radiation. The adaptive boundary conditions ensure that, on the one hand, waves freely go out of the model domain and, on the other hand, the external conditions influence the solution within the domain. The numerical experiment performed for a 17-year model time indicates that the model solution reaches a statistically quasi-periodic regime.

Comparative analysis of the model solution and observational data for the area of the Hawaiian Islands shows that the model can realistically reproduce averaged parameters of the ocean state. The model is also capable of reproducing the variability of the ocean state and, first and foremost, such key characteristics
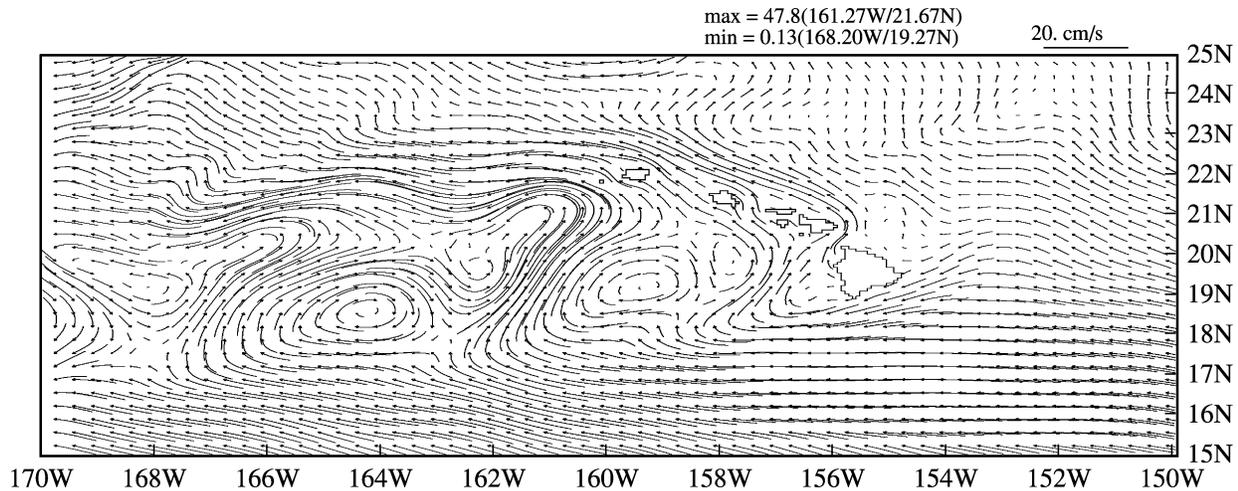
max = 47.8(161.27W/21.67N)
min = 0.13(168.20W/19.27N)
20. cm/s

Fig. 8. Streamlines of currents at a depth of 2 m for 00:00 of November 16 model time. A maximum velocity of 47.8 cm/s is reached at the point (161.27°W, 21.67°N). A model solution.
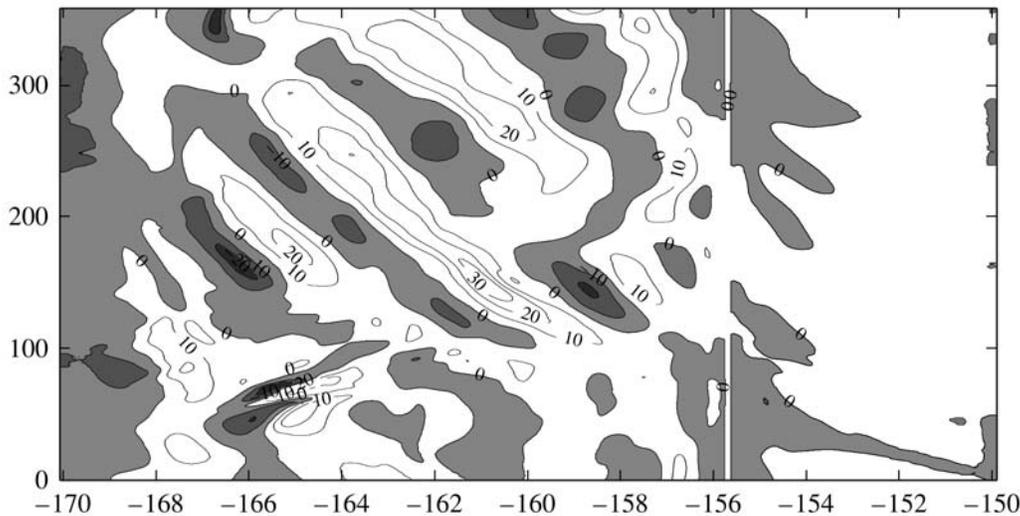
Fig. 9. Time–longitude cut of the meridional velocity component along 19°N at a depth of 25 m. Positive velocities indicate a northward direction. The axis of abscissa denotes longitude, and the axis of ordinates denotes time in days. A model solution.

for the understanding of water circulation in the area of the islands as the dynamics of eddies on a synoptic spatiotemporal scale. The model reveals the generation of synoptic eddies at NEC velocity shears, when the current impinges upon the ridge of islands, and the transport of these eddies to the west, in accordance with observational data. The rates of eddy propagation estimated from the model and altimetric measurements are close to each other.

The model solution includes an element of circulation important for estimating the currents in the area west of the Hawaiian Islands, namely, a northward current in the upper oceanic layer. This current clearly manifests itself in averaged fields. The averaged currents also indicate that, between the islands of Hawaii and Maui, as well as between the islands of Molokai

and Oahu, the upper 100–150-m layer is characterized by water transport from the west to east side of the ridge of islands.

The proposed model and the results obtained on its basis can be used in systems of operative monitoring for limited areas of the ocean.

APPENDIX

MODEL OF OCEAN HYDRODYNAMICS

1. Equations of Ocean Hydrodynamics Model

The state of sea hydrodynamics is described by three-dimensional functions of temperature, salinity, and components of current velocity and by a two-

dimensional function of the sea surface height. The model of sea hydrodynamics involves three-dimensional primitive equations of geophysical fluid dynamics [15–17].

The model equations are formulated in a spherical system of coordinates: λ is the latitude, φ is the longitude, and z is the depth. The z axis is directed vertically downward, and, for the undisturbed sea surface, it is assumed that $z = 0$. The problem is solved in a three-dimensional domain Ω. The domain boundary is the surface G, where $G = G_H \cup G_\zeta \cup G_S \cup G_O$. G_H is the lower boundary described by the function $z = H(\lambda, \varphi)$, where $H(\lambda, \varphi)$ is a two-dimensional positive function describing the sea-bottom topography. G_S and G_O are the lateral boundaries. G_S is the solid lateral boundary and G_O is the open lateral boundary of the domain. The upper boundary of the domain G_ζ is movable and described by the equation $z = -\zeta(\lambda, \varphi, t)$, where $\zeta(\lambda, \varphi, t)$ is the deviation of the sea surface from the undisturbed oceanic surface $z = 0$.

The system uses the Boussinesq and hydrostatic approximations and may be written as follows:

$$u_t + (\mathbf{v} \cdot \nabla)u + wu_z - fv + a^{-1}\tan\varphi u^2$$
$$= -(\rho_0 a \cos\varphi)^{-1} p_\lambda + (K_m u_z)_z + D_u, \tag{1}$$

$$v_t + (\mathbf{v} \cdot \nabla)v + wv_z + fu + a^{-1}\tan\varphi uv$$
$$= -(\rho_0 a)^{-1} p_\varphi + (K_m v_z)_z + D_v, \tag{2}$$

$$p_z = \rho g, \tag{3}$$

$$\nabla \mathbf{v} + w_z = 0, \tag{4}$$

$$T_t + (\mathbf{v} \cdot \nabla)T + wT_z$$
$$= (K_h T_z)_z + D_T + (\rho_0 c_p)^{-1} I_z (1 - A), \tag{5}$$

$$S_t + (\mathbf{v} \cdot \nabla)S + wS_z = (K_h S_z)_z + D_S, \tag{6}$$

$$\rho = \rho(T, S). \tag{7}$$

In Eqs. (1)–(7), the following notation is used: $\mathbf{v} = (u, v)$ is the vector of horizontal wind components; w is the vertical velocity component; ρ is density; ρ_0 is the seawater density averaged over the model domain; $f = 2\Omega_E \sin\varphi$ is the Coriolis parameter, where Ω_E is the angular velocity of the Earth's rotation; $\nabla\eta = (a\cos\varphi)^{-1}[(u\eta)_\lambda + (v\eta\cos\varphi)_\varphi]$ is a two-dimensional gradient operator; K_m and K_h are the coefficients of vertical turbulent viscosity and diffusion, respectively; a is the Earth's radius; D_u, D_v, D_T, and D_S are the terms describing the horizontal turbulent viscosity and diffusion of heat and salinity, respectively; I is the flux of penetrative solar radiation; and A is the sea-ice compactness. In the general case, the

coefficient of vertical turbulent viscosity may be variable.

The equation of state for water is given according to [32].

The horizontal turbulent viscosity is described by the operator

$$D_\eta \eta = A_m \Delta\eta + A_m^2 \Delta^2\eta, \tag{8}$$

where $\Delta\eta = (a\cos\varphi)^{-1}[(a\cos\varphi)^{-1}(\eta_\lambda)_\lambda + a^{-1}(\eta_\varphi\cos\varphi^{-1})_\varphi]$ denotes one of the functions u and v and A_m and A_m^2 are coefficients.

The horizontal turbulent diffusion of heat and salinity is described by the operator

$$D_\eta \eta = A_h \Delta\eta, \tag{9}$$

where η denotes one of the functions T and S and A_h is the coefficient of horizontal turbulent diffusion of heat.

Under stable stratification conditions, the coefficients of vertical turbulent viscosity and diffusion are calculated by the Munk–Anderson model [33]

$$K_m = a_{m0}/(1 + \alpha_{MA}\text{Ri})^n + a_{mb}$$
$$K_h = a_{h0}/(1 + \alpha_{MA}\text{Ri})^n + a_{hb}, \tag{10}$$

where a_{m0}, a_{mb}, a_{h0}, a_{hb}, α, and n are empirical constants and $\text{Ri} = g\rho_0^{-1}\rho_z/(u_z)^2 + (v_z)^2]$ is the Richardson number. The parameters a_{mb} and a_{hb} describe the minimum values of the coefficients K_m and K_h, respectively; and the parameters α_{MA} and n describe the sensitivity of K_m and K_h to the Richardson number.

The convective mixing, which arises in the case of unstable stratification, is parameterized in the model by averaging the temperature and salinity of unstable layers with conservation of the total amount of heat and salt.

2. Boundary Conditions

The dynamics of the upper sea boundary with consideration for the mass flux is described by the equation of the free sea surface

$$w + \zeta_t = \rho_f^{-1} W, \tag{11}$$

where ρ_f is the density of fresh water, and W is the intensity of water flow in the sea [kg s^{-1} m^{-2}], which is defined by precipitation, evaporation, melting, and ice freezing.

The boundary conditions at the air–sea interface are set for the sea surface $z = -\zeta(\lambda, \varphi, t)$:

$$-K_m(u_z, v_z) + (u, v)\rho_f^{-1} W = \rho_0^{-1}(1 - A)(\tau^\lambda, \tau^\varphi), \tag{12}$$

$$p = p_a, \qquad (13)$$

$$-c_p K_h T_z + c_p T \rho_f^{-1} W = \rho_0^{-1}[Q_h^{aw}(1 - A) + Q_h^{iw} A], \quad (14)$$

$$-K_h S_z + S \rho_f^{-1} W = \rho_0^{-1} S^{iw} M A. \qquad (15)$$

In conditions (12)–(15), $\tau^\lambda(\lambda, \varphi, t)$, $\tau^\varphi(\lambda, \varphi, t)$ is the wind stress; $Q_h^{aw}(\lambda, \varphi, t)$ is the heat flux at the air–sea interface; $Q_h^{iw}(\lambda, \varphi, t)$ is the heat flux at the water–ice interface; c_p is the heat capacity of seawater; and $S^{iw} M$ is the intensity of salt emission into the sea during ice freezing and melting.

The model assumes that the sea bottom consists of piecewise-constant surfaces and the lateral boundaries are vertical surfaces. At the sea bottom $z = H(\lambda, \varphi)$, the boundary conditions are as follows:

$$w = u(a \cos\varphi)^{-1}\frac{\partial H}{\partial \lambda} + v a^{-1}\frac{\partial H}{\partial \varphi}, \qquad (16)$$

$$-\rho_0 K_m \frac{\partial(u, v)}{\partial z} = (\tau_B^\lambda, \tau_B^\varphi), \qquad (17)$$

$$-\rho c_p K_h \frac{\partial T}{\partial z} = 0, \qquad (18)$$

$$-\rho K_h \frac{\partial S}{\partial \mathbf{n}} = 0. \qquad (19)$$

In condition (17), $\tau_B^\lambda(\lambda, \varphi, t)$ and $\tau_B^\varphi(\lambda, \varphi, t)$ are the zonal and meridional components of bottom friction stress. The parametrization of the bottom friction stress can be found in [19].

At the solid lateral boundaries (G_S), the no-flow and free-slip conditions are imposed and the fluxes of heat and salt are assumed to be zero.

At the open boundaries, we set adaptive conditions based on the wave equation [30]. This method allows the waves to freely go out of the internal area through the open boundaries, independent of the direction of advective transport, and to transmit information (large-scale characteristics) from the external (with respect to the given domain) area into the inner domain.

The wave equation includes both the normal and tangential (to the boundary) components of the phase velocity [34]:

$$\frac{\partial f}{\partial t} + c_x \frac{\partial f}{\partial x} + c_y \frac{\partial f}{\partial y} = -c_x \frac{1}{\tau}(f - f^{\text{ext}}), \qquad (20)$$

where (c_x, c_y) is the phase velocity of transport along the normal and tangential (to the boundary) components in Cartesian coordinates (x, y) and is calculated from the solution in the area adjacent to the open boundary. Equation (20) is nonlinear. An important distinction between the two-dimensional wave equation and the one-dimensional wave equation normal to the boundary (which was considered in [35]) is a more accurate calculation of the phase velocity of transport. In [34], it has been demonstrated that, in the one-dimensional case, the phase velocity normal to the boundary c_x may oscillate between large positive and negative values.

At the solid lateral and open boundaries, the following condition is imposed for the biharmonic operator:

$$\Delta u = \Delta v = 0. \qquad (21)$$

The initial conditions for the system are

$$(u, v, T, S, \zeta)|_{t = 0} = (u^0, v^0, T^0, S^0, \zeta^0). \qquad (22)$$

A detailed description of finite-difference schemes for solving the model equations can be found in [18, 19, 21].

REFERENCES

1. V. G. Bondur, *Aerospace Methods in Modern Oceanology*, Ed. by M. E. Vinogradov and S. S. Lappo (Nauka, Moscow, 2004), pp. 55–117 [in Russian].

2. V. G. Bondur, "Complex Satellite Monitoring of Coastal Water Areas," in *Proceedings of 31 International Symposium on Remote Sensing of Environment* (St. Petersburg, 2005).

3. *Atlas of Oceans. Pacific Ocean*, Ed. by S. G. Gorshkov (USSR Ministry of Defense, Moscow, 1974) [in Russian].

4. *Atlas of Hawaii*, Ed. by S. P. Juvik and J. O. Juvik (Univ. of Hawaii Press, Honolulu, 1998).

5. W. White, "A Narrow Boundary Current along the Eastern Side of the Hawaiian Ridge: The North Hawaiian Ridge Current," J. Phys. Oceanogr. **13**, 1726–1731 (1983).

6. J. M. Price, M. L. Van Woert, and M. Vatousek, "On the Possibility of a Ridge Current along the Hawaiian Islands," J. Geophys. Res. C **99**, 14 101–14 112 (1994).

7. F. M. Bingham, "Evidence for the Existence of a North Hawaiian Ridge Current," J. Phys. Oceanogr. **28**, 991–998 (1998).

8. E. Firing, "Currents Observed North of Oahu during the First Five Years of HOT," Deep-Sea Res. **43**, 281–303 (1996).

9. E. Firing, B. Qiu, and W. Miao, "Time-Dependent Island Rule and Its Application to the Time-Varying North Hawaiian Ridge Current," J. Phys. Oceanogr. **29**, 2671–2688 (1999).

10. B. Qiu, D. A. Koh, and C. Lumpkin, "Flament. P. Existence and Formation Mechanism of the North Hawaiian Ridge Current," J. Phys. Oceanogr. **27**, 431–444 (1997).

11. W. C. Patzert, *Eddies in Hawaiian Waters* (Hawaii Inst. of Geophysics, Hawaii, 1969), No. 69-08.

12. G. T. Mitchum, "The Source of 90-Day Oscillations at Wake Island," J. Geophys. Res. C **100**, 2459–2475 (1995).

13. C. L. Holland and G. T. Mitchum, "Propagation of Big Island Eddies," J. Geophys. Res. C **106**, 935–944 (2001).

14. P. Flament, *Ocean Atlas of Hawaii* (1996); http://radlab.soest.hawaii.edu/atlas/currents.html

15. A. S. Sarkisyan, *Principles of Theory and Calculation of Ocean Currents* (Gidrometeoizdat, Leningrad, 1966) [in Russian].

16. A. S. Sarkisyan, *Numerical Analysis and Prediction of Sea Currents* (Gidrometeoizdat, Leningrad, 1977) [in Russian].

17. K. Bryan, "A Numerical Method for the Study of the Circulation of the World Ocean," J. Comput. Phys. **4**, 347–376 (1969).

18. Yu. L. Demin and R. A. Ibrayev, "Model of Ocean Dynamics," in *Numerical Models and Results of Calibration Calculations of Currents in the Atlantic Ocean* (Inst. of Numerical Mathematics of the Russian Academy of Sciences, Moscow, 1992), pp. 42–95 [in Russian].

19. R. A. Ibraev, "Reconstruction of Climatic Characteristics of the Gulf Stream techeniya Gol'fstrim," Izv. Akad. Nauk, Fiz. Atmos. Okeana **29**, 803–814 (1993).

20. A. S. Sarkisyan, "Analysis of Model Calibration Results: Atlantic Ocean Climatic Calculations," J. Mar. Syst. **5**, 47–66 (1995).

21. R. A. Ibrayev, "Model of Enclosed and Semi-Enclosed Sea Hydrodynamics," Russ. J. Numer. Anal. Math. Model. **16**, 291–304 (2001).

22. ETOPO2. http://www.ngdc.noaa.gov/mgg/fliers/01mgg04.html

23. WOA2001. World Ocean Atlas 2001. High resolution (1/4 degree) Temperature and Salinity Analyses of the World's Oceans. Version 2. http://www.nodc.noaa.gov/OC5/WOA01/

24. F. Roske, *An Atlas of Surface Fluxes Based on the ECMWF Re-Analysis—A Climatological Dataset to Force Global Ocean General Circulation Models* (Max-Planck-Inst. fur Meteorologie, Hamburg, 2001).

25. J. K. Gibson, P. Kallberg, S. Uppala, et al., *ERA-15 Description* (Version 2), ECMEF Re-Analysis Project Report Series, No.1 (1999).

26. G. I. Marchuk and B. A. Kagan, *Dynamics of Ocean Tides* (Gidrometeoizdat, Leningrad, 1983) [in Russian].

27. A. Gill, *Atmosphere–Ocean Dynamics* (Academic, New York, 1982; Mir, Moscow, 1986).

28. D. Praudman, *Dynamic Oceanography* (Wiley, London, 1953; Inostrannaya Literatura, Moscow, 1957).

29. A. L. Perkins, L. F. Smedstad, D. V. Blake, et al., "A New Nested Boundary Condition for a Primitive Equation Ocean Model," J. Geophys. Res. C **102**, 3483–3500 (1997).

30. P. Marschesiello, J. C. McWilliams, and A. Shchepetkin, "Open Boundary Conditions for Long-Term Integration of Regional Oceanic Models," Ocean Model. **3**, 1–20 (2001).

31. K. Wyrtki, "Eddies in the Pacific North Equatorial Current," J. Phys. Oceanogr. **12**, 746–749 (1982).

32. UNESCO. Seventh Report of the Joint Panel on Oceanographic Tables and Standards, UNESCO Techn. Papers. Mar. Sci., No. 24, 39–54 (1976).

33. W. H. Munk and E. R. Anderson, "Note on the Theory of the Thermocline," J. Mar. Res. **7**, 276–295 (1948).

34. W. H. Raymond and H. L. Kuo, "A Radiation Boundary Condition for Multi-Dimensional Flows," Q. J. R. Meteorol. Soc. **110**, 535–551 (1984).

35. I. Orlansky, "A Simple Boundary Condition for Unbounded Hyperbolic Flows," J. Comput. Phys. **21**, 251–269 (1976).